Correlation Matching Approach for Through-Wall Corner Detection

Eva Lagunas[1], Moeness G. Amin[2], Fauzia Ahmad[2] and Montse Nájar[1]
[1] Department of Signal Theory and Communications, Universitat Politècnica de Catalunya (UPC), 08034 Barcelona, Spain
[2] Radar Imaging Lab, Center for Advanced Communications, Villanova University, Villanova, PA 19085, USA

***Abstract*—We consider the problem of detecting building dominant scatterers using Compressive Sensing (CS) with applications to through-the-wall radar and urban sensing. We use oblique illumination, which specially enhances the radar returns from the corners formed by the orthogonal intersection of two walls. This paper uses a novel type of image descriptor: the intensity correlogram. The intensity correlogram of each through-the-wall radar image pixel encodes information about spatial correlation of intensities. The proposed technique compares the known intensity correlogram of the scattering response of an isolated canonical corner reflector with the correlogram of the received radar signal within a correlation matching framework. The correlation matching procedure directly promotes sparse solution avoiding solving the l_1-norm constrained optimization problem encountered in conventional CS.**

I. Introduction

Sensing through building walls using RF signals to gain vision into concealed scenes is the aim of Through-the-Wall Radar Imaging (TWRI) [1]–[4]. The ability to remotely and reliably detect the presence of humans and objects of interest through opaque structures has numerous applications in civilian, law enforcement and military sectors [5]. TWRI combines electromagnetic waves transmitted and received at several different antenna locations along an array aperture, either real or synthesized, to obtain 2D or 3D images of the region of interest located behind the front wall.

In this paper, we address the problem of detecting building interior structures for TWRI applications. Doppler signatures or change detection techniques cannot be applied since the targets of interest and clutter are both of the same nature. Usually, stationary target detection is performed subsequent to image formation [2]. In that sense, the through-the-wall (TWR) image should contain strong target returns to aid in their detection, localization, and classification. Whether these tasks are performed on pre- or post-processing basis, known target RCS can both guide the operational concept and the selection of proper system parameters, leading to efficient and high performance imaging. Testimonial to this fact is the entire subject of matched illumination and waveform design [6], [7]. Operational concept can include less constrained data collection strategies, including decisions on the required number and placements of physical antennas or configuration of a synthesized aperture. This paper considers the operational concept, rather than waveform design, to improve detection of walls and their boundaries. Image-based processing for determining the building interior structure faces many challenges, impeding the application of likelihood ratio detection.

Unlike majority of the feature detection methods that are applied in the image domain, the proposed approach exploits prior information of building construction practices. The building layout is usually composed of exterior and interior walls which are parallel or perpendicular to each other. We assume a flexibility in radar operation which allows proper angular radar illuminations, thereby avoiding the front wall returns and preserving the corner features created by the junction of walls of a room. This can be achieved using squint beamforming or broadside beams with tilted aperture [8]. Estimating dominant scatterers such as corners allows the inference of building interior structure. This same idea was exploited in [9]–[11], where a building feature based approach was applied to estimate the type and location of different canonical scattering mechanisms. This paper uses a novel type of image descriptor: the intensity correlogram. The intensity correlogram of each through-the-wall radar image pixel encodes information about spatial correlation of intensities. The basic strategy adopted here is to compare the known intensity correlogram of the scattering response of an isolated canonical corner reflector with the correlogram of the received radar signal within a correlation matching framework. The correlation matching procedure directly promotes sparse solution avoiding solving the l_1-norm constrained optimization problem encountered in conventional CS. The feature-based nature of the proposed detector enables corner separation from other indoor scatterers such as furniture or humans. Simulation results show that the use of spatial intensity correlation makes the detection performance superior to that of using raw signal matching or image matching.

The remainder of this paper is structured as follows. In Section II, the TWR signal model and the canonical corner response are introduced. Section III provides details of the compressive sensing data acquisition. Section IV presents the proposed correlogram based strategy together with other matching techniques for corner detection. Finally, Section V presents simulation results, and Section VI states the conclusions.

This work was partially supported by the Spanish Ministry of Science and Innovation (Ministerio de Ciencia e Innovación) under project TEC2011-29006-C03-02 (GRE3N-LINK-MAC), by the European Commission in the framework of the FP7 Network of Excellence in Wireless COMmunications NEWCOM# (Grant agreement no. 318306), by the Catalan Government under grant 2009 SGR 891 and by the European Cooperation in Science and Technology under project COST Action IC0902.

II. TWR Signal Model

We consider, for simplicity, a monostatic N-element synthetic line array. However, the concept can easily be extended to 2D and/or bistatic arrays. We assume that the data acquisition is carried in an oblique position, which significantly attenuates wall effects and enhances corner scatterers. Let the n-th transceiver illuminate the scene with a stepped frequency signal. The response of the scene can be modeled as the sum of responses from individual scatterers. Thus, the signal received by the n-th transceiver at the m-th frequency can be represented as,

$$y(n,m) = \sum_{p=1}^{P} S_p(n,m,\bar{\phi}_p) e^{-j\omega_m \tau_{p,n}} + w(n,m) \quad (1)$$

where P is the number of scatterers of interest present in the illuminated scene, $\tau_{p,n}$ are the two-way traveling time of the signal from the n-th antenna to the p-th scatterer, $\bar{\phi}_p$ denotes the orientation angle of the p-th scatterer and ω_m is defined as $\omega_m = \omega_0 + m\Delta_\omega$ with $m = 0, \ldots, M-1$ where ω_0 and Δ_ω denote the lowest frequency in the bandwidth spanned by the stepped-frequency signal, and the frequency step size, respectively. The term $w(n,m)$ models the contributions of other scatterers different from those of interest, including the walls and possible multipath propagation effects. The scattering model $S_p(n,m,\bar{\phi}_p)$ is determined in great measure by the geometry of the scatterer. The canonical scattering response of a corner reflector is given by,

$$S_r(n,m,\bar{\phi}_r) = A_r \text{sinc}(\omega_m \frac{L_r}{c} \sin(\phi_{r,n} - \bar{\phi}_r)) \quad (2)$$

The variables A_r, L_r and $\phi_{r,n}$, respectively, define the amplitude, the length and the aspect angle associated with the r-th corner reflector and the n-th antenna.

A radar image is generated from the MN observations, $y(m,n)$, $m = 0, \ldots, M-1$, $n = 0, \ldots, N-1$, using a wideband synthetic aperture beamformer as follows. The scene being imaged is partitioned into a finite number of pixels, $N_x \times N_z$, in crossrange and downrange. That is, the scene can be represented by the complex reflectivity function $r(k,l), k = 0, \ldots, N_x - 1, l = 0, \ldots, N_z - 1$. The complex composite signal, corresponding to the (k,l)th pixel, is obtained by applying a set of focusing delays, $\tau_{(k,l),n}$, to align all signal returns from the (k,l)th pixel, and then summing the results [1],

$$r(k,l) = \frac{1}{MN} \sum_{n=0}^{N-1} \sum_{m=0}^{M-1} y(m,n) e^{j\omega_m \tau_{(k,l),n}} \quad (3)$$

Note that the focusing delay, $\tau_{(k,l),n}$ corresponds to the two-way signal propagation time between the nth antenna location and the (k,l)th pixel. The process described by eqn. (3) is performed for all $N_x \times N_z$ pixels to generate the image of the scene. The aforementioned image formation procedure is commonly known as frequency-domain backprojection.

III. Compressive Sensing in TWRI

Conventional CS-based TWRI has been applied to recover the image of the through-the-wall scene from a reduced number of measurements assuming that the scene itself is sparse, i.e. the scene contains a small number of point like targets. Here, we consider the sparsity described by corners only, improving the conventional point scatterer image sparsity, thus allowing determination of corner locations with a reduced amount of data.

With the aim of compact notation we consider the measurement matrix $\mathbf{Y}$ corresponding to all N antennas defined as,

$$\mathbf{Y} = \begin{bmatrix} \mathbf{y}_0 & \mathbf{y}_1 & \cdots & \mathbf{y}_{N-1} \end{bmatrix}^T \quad (4)$$

where $\mathbf{y}_n$ expresses the received signal corresponding to the nth antenna.

The expression in (4) involves the full set of measurements made at the N array locations using the M frequencies. According to CS, it is possible to recover the corner positions from a reduced set of measurements. Consider $\hat{\mathbf{Y}}$,which is a $Q_n \times Q_m$ ($Q_n < N$ and $Q_m < M$) matrix consisting of elements chosen from $\mathbf{Y}$ as follows,

$$\hat{\mathbf{Y}} = \mathbf{\Phi} \mathbf{Y} \mathbf{\Psi}^T \quad (5)$$

where $\mathbf{\Phi}$ is a $Q_n \times N$ measurement matrix constructed by uniformly at random selecting Q_n rows of an $N \times N$ identity matrix, and $\mathbf{\Psi}$ is a $Q_m \times M$ measurement matrix constructed by uniformly at random selecting Q_m rows of an $M \times M$ identity matrix. We note that $\mathbf{\Phi}$ determines the reduced antenna locations, whereas $\mathbf{\Psi}$ determines the reduced set of frequencies measurements.

IV. Corner Detection Strategies

This section describes different matching-based techniques for estimation of the location of corner scatterers. Corners appear in building structures as a result of the right angle intersection between two walls. We take advantage of the prior knowledge of the corner scattering model by using it as a template or reference for corner recognition.

A. Raw Data Matching

A simple matching approach can be developed in the raw data domain. In this case, the most natural matching function is the Euclidean distance. The detection problem in the raw data domain can be written as,

$$\min_{\sqrt{\beta(k,l)}} d^2 \left(\hat{\mathbf{y}}, \sqrt{\beta(k,l)} \hat{\mathbf{y}}^{\text{ref}}_{(k,l)} \right) \quad (6)$$

where $\hat{\mathbf{y}}$ and $\hat{\mathbf{y}}^{\text{ref}}_{(k,l)}$ denote the compressed received data (in a vector of size $Q_n Q_m$) and the compressed reference signal corresponding to a canonical corner located in the (k,l)-th pixel.

Thus, the solution to (6) is given by,

$$\sqrt{\beta_{DM}(k,l)} = \frac{{\hat{\mathbf{y}}^{\text{ref}}_{(k,l)}}^H \hat{\mathbf{y}}}{{\hat{\mathbf{y}}^{\text{ref}}_{(k,l)}}^H \hat{\mathbf{y}}^{\text{ref}}_{(k,l)}} \quad (7)$$

B. Image Matching

Another possible approach is to directly match the reference image (obtained from the canonical corner data model) from the backprojection image obtained with the observations.

With the values of the illuminated scene image obtained from the compressive measurements lexicographically ordered into a column vector $\hat{\mathbf{r}}$ of length $N_x N_z$, and the values of the image corresponding to the compressive measurements of a canonical corner at position (k,l), denoted as $\hat{\mathbf{r}}^{\text{ref}}_{(k,l)}$, the detection problem can be written as,

$$\min_{\sqrt{\beta}(k,l)} d^2\left(\hat{\mathbf{r}}, \sqrt{\beta(k,l)}\hat{\mathbf{r}}^{\text{ref}}_{(k,l)}\right) \tag{8}$$

Thus, the solution to (8) is given by,

$$\sqrt{\beta_{IM}(k,l)} = \frac{\hat{\mathbf{r}}^{\text{ref}}_{(k,l)}{}^{H}\mathbf{r}}{\hat{\mathbf{r}}^{\text{ref}}_{(k,l)}{}^{H}\hat{\mathbf{r}}^{\text{ref}}_{(k,l)}} \tag{9}$$

C. Intensity Correlogram Matching

We propose a new intensity feature for scatterer detection called intensity correlogram (henceforth correlogram), which expresses how the spatial correlation of pairs of pixel intensities changes with distance. For a pixel (k,l), let $\hat{r}(k,l)$ denote its intensity. For convenience, we use L_∞-norm to measure the distance between pixels, i.e., for pixels (k_1,l_1) and (k_2,l_2), we define the distance between them as $\max\{|k_1-k_2|, |l_1-l_2|\}$. Thus, each distance define a set of pixels equidistant from the reference pixel. Let a distance d be fixed a priori and let the set of pixels intensities of the pixels located at distance d from the reference pixel be denoted as $\hat{r}^{(d)}(k,l)$. Then, the correlogram of a particular pixel $\hat{r}(k,l)$ is defined as,

$$\gamma^{(d)}_{(k,l)} \triangleq \frac{1}{N_p}\sum_{i=1}^{N_p} \hat{r}(k,l)\mathbf{conj}(\hat{r}^{(d)}(k_i,l_i)) \tag{10}$$

From (10) we can built the correlogram matrix defined as,

$$R_{(k,l)} \triangleq \begin{bmatrix} \mathbf{conj}(\gamma^{(d=0)}_{(k,l)}) & \gamma^{(d=1)}_{(k,l)} & \cdots & \gamma^{(d=D-1)}_{(k,l)} \\ \mathbf{conj}(\gamma^{(d=1)}_{(k,l)}) & \gamma^{(d=0)}_{(k,l)} & \cdots & \gamma^{(d=D-2)}_{(k,l)} \\ \vdots & \vdots & \ddots & \vdots \\ \mathbf{conj}(\gamma^{(d=D-1)}_{(k,l)}) & \mathbf{conj}(\gamma^{(d=D-2)}_{(k,l)}) & \cdots & \gamma^{(d=0)}_{(k,l)} \end{bmatrix} \tag{11}$$

which is positive semidefinite.

The isolated presence of a canonical corner in the (k,l)-th pixel will generate a particular reference correlogram matrix which is denoted as $\mathbf{R}^{\text{ref}}_{(k,l)}$. The proposed procedure is based on a scan which reacts only when the reference scatterer is present.

Let the sample correlogram matrix obtained from the compressed observations $\hat{y}(n,m)$ for a particular pixel (k_p,l_p) be denoted as $\hat{\mathbf{R}}_{(k_p,l_p)}$. If the scene contains a corner at that particular pixel, then,

$$\hat{\mathbf{R}}_{(k_p,l_l)} = \beta(k_p,l_p)\mathbf{R}^{\text{ref}}_{(k_p,l_p)} + \mathbf{R}_w \tag{12}$$

where $\beta(k_p,l_p)$ is an intensity level of the p-th corner located at the (k_p,l_p) pixel.

Based on these assumptions, some similarity function is required to measure the reference corner intensity contained in the given sample correlogram matrix at each (k,l)-th pixel. An estimate of the corner intensity level β can be formulated as,

$$\min_{\beta} \Psi\left(\hat{\mathbf{R}}_{(k,l)}, \beta(k,l)\mathbf{R}^{\text{ref}}_{(k,l)}\right) \tag{13}$$

where $\Psi(\cdot,\cdot)$ is a similarity function between the two matrices. Note that the solution to (13) will be clearly a function of the crossrange (k) and downrange (l).

1) Corner Detector Based on the Frobenius Norm: Let us consider the Frobenius norm as a similarity function $\Psi(\cdot,\cdot)$. The detection problem can be written as,

$$\min_{\beta(k,l)} \left|\hat{\mathbf{R}}_{(k,l)} - \beta(k,l)\mathbf{R}^{\text{ref}}_{(k,l)}\right|_F \tag{14}$$

and the solution to (14) is given by,

$$\beta_F(k,l) = \frac{\text{Trace}\left(\mathbf{R}^{\text{ref}}_{(k,l)}{}^{H}\hat{\mathbf{R}}_{(k,l)}\right)}{\text{Trace}\left(\mathbf{R}^{\text{ref}}_{(k,l)}{}^{H}\mathbf{R}^{\text{ref}}_{(k,l)}\right)} \tag{15}$$

2) Corner Detector Based on the Positive Semidefinite Difference between Correlogram Matrices: A second estimate can be derived by forcing a positive definite difference between the correlogram matrix obtained from the observations and the candidate correlogram matrix.

The problem can be formulated as

$$\begin{aligned} \max_{\beta(k,l)\geq 0} \quad & \beta(k,l) \\ \text{s.t.} \quad & \hat{\mathbf{R}}_{(k,l)} - \beta(k,l)\mathbf{R}^{\text{ref}}_{(k,l)} \succeq 0 \end{aligned} \tag{16}$$

If $\hat{\mathbf{R}}_{(k,l)} - \beta(k,l)\mathbf{R}^{\text{ref}}_{(k,l)}$ must be positive semidefinite, $\mathbf{I} - \beta(k,l)\hat{\mathbf{R}}^{-1}_{(k,l)}\mathbf{R}^{\text{ref}}_{(k,l)}$ must be too. Thus, using the Eigen-Decomposition of $\hat{\mathbf{R}}^{-1}_{(k,l)}\mathbf{R}^{\text{ref}}_{(k,l)}$ defined by $\mathbf{U}\Lambda\mathbf{U}^H$,

$$\mathbf{I} - \beta(k,l)\mathbf{U}\Lambda\mathbf{U}^H \succeq 0 \;\Rightarrow\; \mathbf{I} - \beta(k,l)\Lambda \succeq 0 \tag{17}$$

where Λ is a diagonal matrix whose diagonal elements are the corresponding eigenvalues of the matrix $\hat{\mathbf{R}}^{-1}_{(k,l)}\mathbf{R}^{\text{ref}}_{(k,l)}$. The worst case is given by,

$$\lambda^{-1}_{max}(\hat{\mathbf{R}}^{-1}_{(k,l)}\mathbf{R}^{\text{ref}}_{(k,l)}) - \beta(k,l) = 0 \tag{18}$$

Thus, the solution to (16) is given by the inverse of the maximum eigenvalue of $\hat{\mathbf{R}}^{-1}_{(k,l)}\mathbf{R}^{\text{ref}}_{(k,l)}$, that is,

$$\beta_M(k,l) = \lambda^{-1}_{max}(\hat{\mathbf{R}}^{-1}_{(k,l)}\mathbf{R}^{\text{ref}}_{(k,l)}) \tag{19}$$

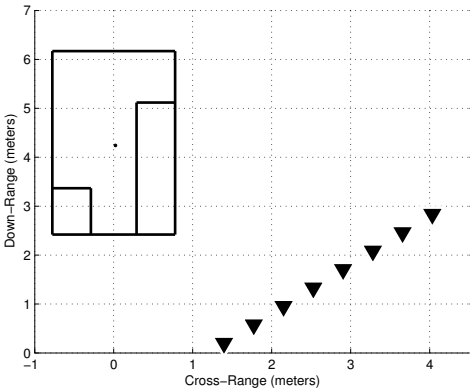

(a)

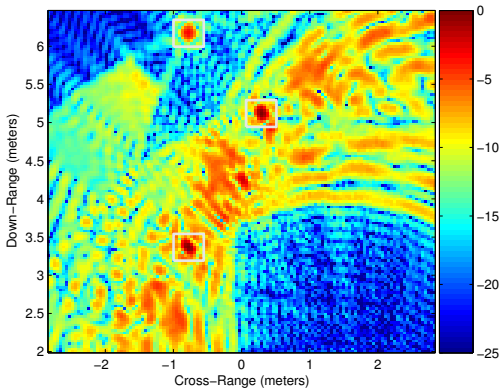

(b)

Fig. 1: (a) Geometry of the simulated scene, (b) Backprojection image of the scene.

V. Simulation Results

A stepped-frequency signal consisting of 335 frequencies covering the 1 to 2 GHz frequency band was used for interrogating the scene. The data acquisition employs monostatic SAR consisting of 8-element locations with an inter-element spacing of 53 cm (1.77λ where λ is the wavelength at 1 GHz). Conventional monostatic SAR theory assumes an antenna spacing smaller than 0.25λ in order to avoid grating lobes within the visible region, -90° to +90°. In our particular scene, the region of interest goes from -23° to +23°, which translates into a maximum antenna spacing equal to 0.36λ. Therefore, the antenna compression rate is $\rho_n = \frac{0.36\lambda}{1.77\lambda} = 0.2$. An oblique illumination of the scene is used to avoid wall returns while preserving the important corner features. The angular tilt of the SAR system is chosen to be 45° so that the corner response of eq. (2) is maximized.

The system illuminates a building consisting of three rooms, as shown in Fig. 1(a), where the geometry of the simulated scene is depicted. In the middle of the building, located at (0.02,4.24)m, there is a point target which emulates the presence of a human. The region to be scanned by the detector is the same as the region to be imaged and is chosen to be 5.64 (cross-range) × 4.45 (down-range) m^2, centered at (0,4.23)m, and is divided into 128 × 128 pixels.

Fig. 1(b) shows the backprojection image corresponding to the measured scene, using all 335 frequencies. In this figure and all subsequent radar figures in this section, we plot the image intensity with the maximum intensity value in each image normalized to 0dB. Although the corners are present in the images (indicated by white rectangles), it is difficult to discern the corner presence from the point target and clutter contribution.

For sparsity-based corner detection, we consider only 34 of the frequencies (uniformly selected frequencies). Therefore, the frequency compression rate is $\rho_f = \frac{34}{335} = 0.10$. Fig. 2(a) and 2(b) show the two images obtained with the proposed correlation matching approach with $D = 30$. Fig. 2(a) corresponds to the minimization of the Frobenius Norm and Fig. 2(b) corresponds to the eigenvalue method. Both images Fig. 2(a) and Fig. 2(b) have less clutter compared to the corresponding backprojection image shown in Fig. 1(b), specially the one obtained with the eigenvalue method. Moreover, the point target has also been diminished due to the feature-based nature of the detector.

For comparison purposes, Fig. 2(c) and Fig. 2(d) show the resulting images obtained applying the matching approach in the raw data domain ($\beta_{DM}(k,l)$) and applying the matching approach in the image domain ($\beta_{DM}(k,l)$), respectively. Both images shown in Fig. 2(c) and Fig. 2(d) are more cluttered than that shown in Fig. 2(b).

A. Target-to-Clutter Comparison

As a performance measure, we use the Target-to-Clutter Ratio (TCR) [12], which is defined as the ratio between the maximum pixel magnitude value of the target to the average pixel magnitude value in the clutter region,

$$TCR = 20\log_{10}\left(\frac{\max_{(k,l)\in A_t}|\beta(k,l)|}{\frac{1}{N_c}\sum_{(k,l)\in A_c}|\beta(k,l)|}\right) \qquad (20)$$

where A_t is the target area, A_c is the clutter area and N_c is the number of pixels in the clutter area. The target area is manually selected in close vicinity to the target (11×11 pixel box centered at the real corner position).

The advantage of the proposed correlogram matching method over backprojection and its competitors is evident in Table I, where the TCR for non-compression ($\rho_f = 1$) are illustrated. We observe from Table I that the proposed correlogram matching with the eigenvalue method provide a significant improvement over the corresponding backprojection results and over its competitors, specially for big values of D. Increasing D gives more information to be compared in the correlation matching, but it also increases the algorithm complexity. The results for different frequency compression are summarized in Table II. The TCR values provided in Table II suggest that the quality of the images obtained with the proposed method does not suffer from the frequency reduction.

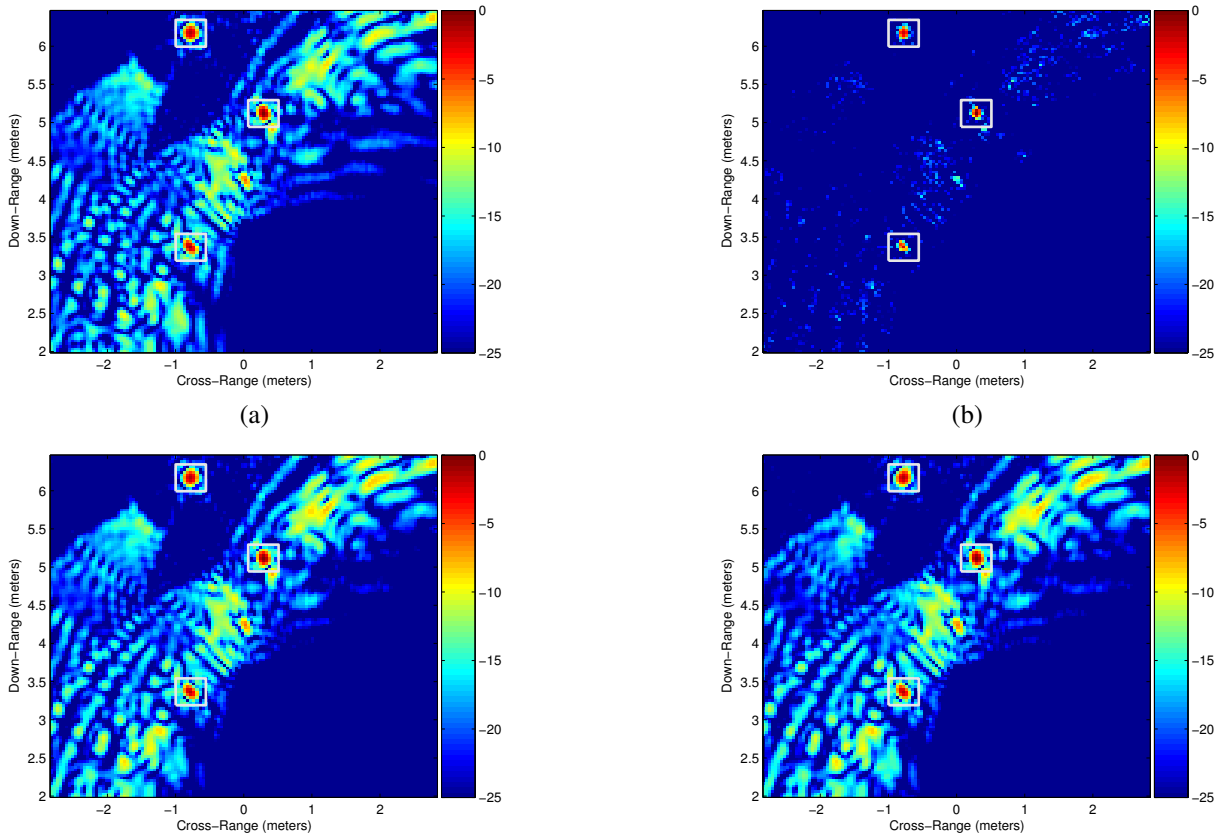

Fig. 2: Resulting images: (a) Correlogram match. - Frobenius norm, (b) Correlogram match. - Eigenvalue method, (c) Raw data match., (d) Image match.

TABLE I: TCR: $\rho_f = 1$

	D=5	D=10	D=15	D=30
Backprojection	14.45 dB			
Raw Data match.	103.53 dB			
Image match.	99.98 dB			
Frobenius norm	105.15 dB	105.49 dB	105.64 dB	105.80 dB
Eigenvalue method	265.15 dB	672.98 dB	933.64 dB	1125.03 dB

TABLE II: TCR: $D = 30$

ρ_f	Eigenvalue method	Frobenius norm
1	1125.03 dB	105.80 dB
0.5	1127.63 dB	106.13 dB
0.25	1125.56 dB	106.03 dB
0.10	1119.48 dB	106.75 dB

VI. Conclusion

In this paper, we developed a corner detector for TWRI applications following a correlation matching framework, where the a priori known intensity correlogram of the scattering response of an isolated canonical corner reflector is compared with the correlogram of the received radar signal within a correlation matching framework. The simulation results have shown that the proposed method significantly reduces clutter, allowing an effective simple thresholding-based detection with improved performance over its backprojection imaging and raw data and image based detector counterparts.

References

[1] M. G. Amin and F. Ahmad, "Wideband Synthetic Aperture Beamforming for Through-the-Wall Imaging," *IEEE Signal Process. Mag.*, vol. 25, no. 4, pp. 110–113, Jul, 2008.

[2] M. G. Amin (Ed.), "Through-the-Wall Radar Imaging," *CRC Press, Boca Raton, FL*, 2010.

[3] M. G. Amin and K. Sarabandi (Eds.), "Special issue on Remote Sensing of Building Interior," *IEEE Trans. Geosci. Remote Sens.*, vol. 47, no. 5, pp. 1270–1420, May, 2009.

[4] F. Soldovieri and R. Solimene, "Through-Wall Imaging Via a Linear Inverse Scattering Algorithm," *IEEE Geosci. Remote Sens. Letters*, vol. 4, no. 4, pp. 513–517, Oct, 2007.

[5] H. Burchett, "Advances in Through Wall Radar for Search, Rescue and Security Applications," *Inst. of Eng. and Tech. Conf. Crime and Security, London, UK*, pp. 511–525, Jun, 2006.

[6] S. Pillai, H. Oh, D. Youla, and J. Guerci, "Optimum Transmit-Receiver Design in the Presence of Signal-Dependent Interference and Channel Noise," *IEEE Trans. Inf. Theory*, vol. 46, no. 2, pp. 577–584, Mar, 2000.

[7] D. Gjessing, *Target Adaptive Matched Illumination RADAR: Principles and Applications, IEE Electromagnetic Waves Series 22*. Peter Peregrinus Ltd., London, UK, 1986.

[8] P. Sevigny and D. DiFilippo, "A Multi-Look Fusion Approach to Through-Wall Radar Imaging," *IEEE Radar Conference, Ottawa, Canada*, Apr, 2013.

[9] E. Lagunas, M. Amin, F. Ahmad, and M. Najar, "Determining Building Interior Structures Using Compressive Sensing," *SPIE Journal of Electronic Imaging*, vol. 22, no. 2, p. 021003, 2013.

[10] N. Subotic, E. Keydel, J. Burns, A. Morgan, K. Cooper, B. Thelen, B. Wilson, W. Williams, S. McCarty, B. Lampe, B. Mosher, and D. Setterdahl, "Parametric reconstruction of internal building structures via canonical scattering mechanisms," *IEEE Int. Conf. Acoustics, Speech and Signal Processing (ICASSP), Las Vegas, USA*, 2008.

[11] E. Ertin and R. Moses, "Through-the-Wall SAR Attributed Scattering Center Feature Estimation," *IEEE Trans. Geosci. Remote Sens.*, vol. 47, no. 5, pp. 1338–1348, May, 2009.

[12] Y. Yoon and M. G. Amin, "Spatial Filtering for Wall-Clutter Mitigation in Through-the-Wall Radar Imaging," *IEEE Trans. Geosci. Remote Sens.*, vol. 47, no. 9, pp. 3192–3208, 2009.